Scalable Construction of Anatomically Detailed Biatrial Models with Personalised Electrophysiology from Imaging or Electroanatomic Mapping Data

Caterina Vidal Horrach[1], Laura Bevis[1], Mahmoud Ehnesh[1], Semhar Misghina[1], Ovais Ahmed Jaffery[1], Carlos Edgar Lopez Barrera[1], Alexander Zolotarev[1], Fuyu Cheng[1], Steven Niederer[2], Edward Vigmond[3], and Caroline Roney[1]

[1] Queen Mary University of London, London, United Kingdom
[2] Imperial College of London, London, United Kingdom
[3] University of Bordeaux

Abstract

Catheter ablation success rates for persistent atrial fibrillation (AF) remain limited, reflecting the complex interplay of anatomical, structural, and functional factors sustaining arrhythmia. Patient-specific biophysical models provide a physics-constrained framework to simulate AF mechanisms and predict individual treatment responses, while large-scale in silico trials enable population-level evaluation. To support clinical translation, models must be generated efficiently and reproducibly. We previously introduced atrialmtk, an open-source, cross-platform pipeline for constructing anatomically detailed atrial models from imaging or electroanatomic mapping (EAM) data. atrialmtk produces meshes with anatomical region labelling, fibre architecture, and transmural variation, and has been applied to cohorts exceeding 1000 geometries. Here, we utilise and extend atrialmtk to compare methods for personalising atrial models using late-gadolinium enhancement (LGE)- MRI and EAM data. LGE-MRI based calibration includes fibrotic remodelling via conduction slowing and replacement fibrosis, while EAM-based approaches compare conduction velocity calibration from activation time maps against bipolar voltage and omnipolar voltage based methods. We further demonstrate model calibration to AF cycle length maps to inform patient-specific simulation studies.

1. Introduction

Success rates for catheter ablation therapy in persistent atrial fibrillation (AF) remain low, in part due to the complex interplay of anatomical, structural and functional factors that contribute to arrhythmia initiation and maintenance. Clinically, it is difficult to isolate the individual contribution of each factor. Patient-specific biophysical models offer a physiology- and physics-constrained framework to simulate AF inducibility and predict responses to multiple treatment strategies for an individual. In parallel, large-scale in silico trials allow for assessment of treatment efficacy across virtual populations.

To translate these cardiac computational models from the research environment to the clinic, models must be constructed quickly, reproducibly and at scale. We previously introduced atrialmtk, an open-source pipeline for building anatomically detailed atrial models from imaging or electroanatomic mapping (EAM) data [1]. This platform generates atrial meshes with regional labelling, fibre architecture, and transmural wall variation. It is user-friendly, cross-platform compatible, and scalable, as demonstrated by its application to a cohort of 1000 geometries for population-based in silico studies.

Anatomical atrial models may be further personalised to incorporate structural and functional information from imaging or EAM data; however, it is challenging to determine the optimal methodology for this personalisation [2]. Here we utilise atrialmtk to build anatomical models from imaging and EAM data and then compare different methods of model calibration as follows. For LGE-MRI data personalisation, we compare different types of fibrotic remodelling including conduction slowing and replacement fibrosis (percolation). For EAM-based calibration, we compare conduction velocity calibration from local activation time maps collected at different pacing cycle lengths to personalisation approaches based on bipolar voltage or omnipolar voltage maps. Finally, we present methodologies for calibrating to AF cycle length maps.

2. Methods

We present here an example workflow to construct patient-specific biatrial models from imaging or electroanatomic mapping data. These models are personalised by integrating different types of fibrotic remodelling or conduction calibration from LGE-MRI or EAM data. Throughout our workflow, we present possible software choices and open-source tools.

2.1. Image Segmentation & Meshing

Segmentation of the left and right atria in MRI or CT data can be performed manually, semi-automatically, or fully automatically. Manual segmentation may use tools like CemrgApp [3], 3DSlicer [4] or ITKSnap [5]. In addition, there are several trained networks available for automated segmentation. The 2024 STACOM bi-atrial segmentation challenge provided a large dataset for training deep learning algorithms to automatically segment the left and right atria from LGE-MRI (https://codalab.lisn.upsaclay.fr/competitions/18516). Our proposed model used an ensemble of 5 residual encoder Unet models [6].

Segmented surface meshes were remeshed to a standard resolution suitable for simulation studies using meshtool software (e.g. 0.3 mm average edge length, https://bitbucket.org/aneic/meshtool).

2.2. Mesh Clipping

We typically use Paraview software to clip atrial meshes using the sphere clipping tool to open atrial meshes at the pulmonary veins, mitral vein (MV), tricuspid valve (TV), superior vena cava (SVC), inferior vena cava (IVC) and coronary sinus (CS, https://www.paraview.org/).

2.3. Mesh Landmarking

To select atrial landmarks, a Python script written using the PyVista library was used to enable the user to click on landmark locations, and these locations were written to text files. For all meshes, general left atrial (LA) landmarks were selected as follows: right superior pulmonary vein (RSPV), right inferior pulmonary vein (RIPV), left inferior pulmonary vein (LIPV), left superior pulmonary vein (LSPV), the tip of the left atrial appendage (LAA), and the base of the LAA. Specific landmarks were selected as follows: (i) on the lateral wall, in line with the LSPV, posterior of the LAA; (ii) on the septal wall, in line with the RSPV (at the fossa ovalis); (iii) at the junction of the LA body and LSPV, at the centre of the posterior wall path; (iv) at the junction of the LA body and RSPV, at the centre of the posterior wall path. For the right atrium (RA), a similar set of landmarking was performed, with all locations shown on the atrialmtk github page (https://github.com/pcmlab/atrialmtk).

2.4. Universal Atrial Coordinates Calculation

The Universal Atrial Coordinate (UAC) system is a standardised framework that enables consistent mapping and visualisation of left or right atrial data in two dimensions. It facilitates the registration of imaging and electroanatomic mapping data across various patient-specific meshes. UACs were calculated for assigning atrial regions, registering fibre fields and mapping data between modalities. This calculation involved solving Laplace's equation on the LA mesh with Dirichlet boundary conditions applied to specific boundary nodes using the openCARP simulator [7]. These boundary nodes were calculated using python scripts within the atrialmtk library. For the LA, the four PVs and LAA were mapped to standardised positions within a unit square using two coordinates: a posterior MV to anterior MV coordinates and a lateral-septal coordinate. Equivalently for the RA, the SVC, IVC, CS and right atrial appendage (RAA) were mapped to standard locations in a unit square.

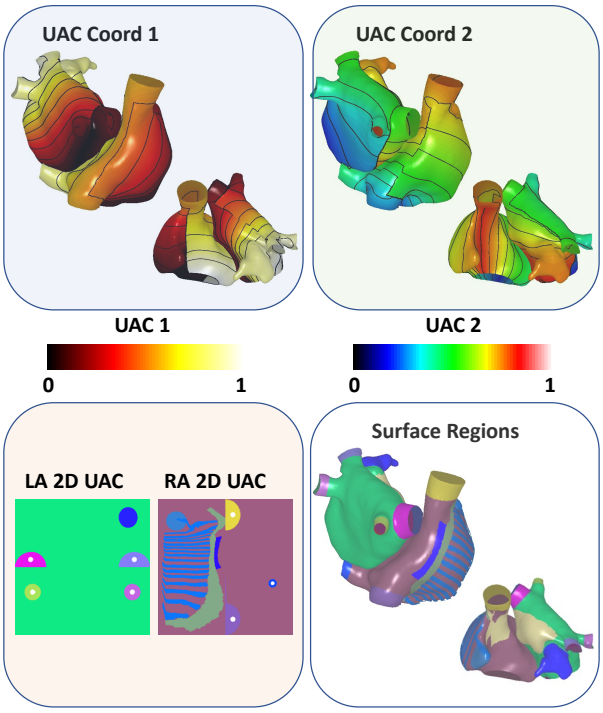

Figure 1. **Universal Atrial Coordinates for a Biatrial Mesh**

2.5. Anatomical Region and Fibre Field Assignment

UACs were used to include atrial structures in the meshes, including crista terminalis, pectinate muscles (PM), Bachmann's bundle (BB) and the sinoatrial node (SAN). These were mapped from an atlas bilayer mesh from Labarthe et al. expressed in UAC [8, 9].

To generate bilayer models, nodes for LA and RA meshes in specific anatomical regions were duplicated and projected endocardially or epicardially. Linear connections were used to connect these structures to their equivalent nodes on the LA or RA epicardial surfaces. Interatrial connections were also added to the meshes at BB, the CS and along the septal wall.

2.6. Electroanatomic Mapping Data Processing

EAM meshes were also converted to UAC using atrialmtk. EAM voltages or activation times for unipolar, bipolar and omnipolar electrogram signal recordings were interpolated to all nodes on the mesh using either Radial Basis Function (RBF) interpolation or Gaussian Process Manifold Interpolation (GPMI). Radial Basis Function (RBF) interpolation was implemented using SciPy's Rbf function in Python, with the inverse multiquadric RBF. The GPMI method uses a Gaussian Process framework, utilising geodesic distances along the manifold to improve interpolation accuracy for complex surfaces. For GPMI, we used an open-source github toolbox ([10], https://zenodo.org/records/5035230).

2.7. AF Simulations

Simulations were run using openCARP simulator with the Courtemanche et al. ionic cell model and the monodomain model for tissue propagation [7]. Following our previous publication, the ionic conductances of the Courtemanche et al. cell model were modified to reproduce physiological heterogeneity between regions of the atria [11, 12]. AF was automatically initiated by seeing four spiral wave re-entries [13]. Transmembrane potential signals were post-processed to calculate phase and phase singularity density maps [14].

2.8. LGE-MRI Fibrosis Modelling: Conduction Slowing & Replacement Fibrosis

To include fibrosis in meshes constructed from LGE-MRI, we projected maximum intensities calculated along surface normals to the mesh and divided these by the mean intensity of the blood pool to obtain image intensity ratio (IIR) values across the mesh.

For conductivity changes, tissue-level conductivities were modified according to IIR thresholds as follows: IIR < 0.9: 0.4 S/m (CV: 0.81 m/s), $0.9 <$IIR< 1.4: 0.31 S/m (CV: 0.74 m/s) $1.4 <$IIR< 1.6: 0.28 S/m (CV: 0.71 m/s), $1.6 <$IIR:0.19 S/m (CV: 0.58 m/s) [15]. For ionic changes, ionic conductances were modified in regions with an IIR> 1.2. Replacement fibrosis was modelled by probabilistically removing elements depending on IIR using a percolation approach [16].

2.9. EAM Fibrosis Modelling: CV Calibration & Voltage Mapping

Each triangular element of the mesh was assigned a peak-to-peak bipolar voltage (BV) value or omnipolar voltage value through interpolation. Voltage models included three types of fibrosis: conductivity changes, ionic changes and replacement fibrosis i.e., percolation [17, 18]. These changes were implemented individually, or in combination using the voltage maps, depending on different voltage thresholds.

For conduction velocity (CV) calibration, a CV field was first calculated from EAM local activation times across the mesh by using the gradient method [19]. A continuous mapping between CV and monodomain conductivity tensor parameters was calculated through running 2D strip simulations for a range of conductivity values, and applied to each element of the mesh.

2.10. EAM Calibration: AF Cycle Length Maps

AF cycle length (AFCL) was calculated for each unipolar signal using autocorrelation by calculating the time interval shift that corresponds to the highest correlation in the signal. These AFCL values were then spatially mapped across all nodes on the atrial surface using GPMI, which accounts for sparse and noisy data [10]. Ionic conductances of the Courtemanche et al atrial cell model were systematically adjusted so that the simulated AFCL reproduced the mean clinical AFCL.

3. Conclusion

Patient-specific models can be personalized using imaging or electroanatomic mapping data, measured for different rates and rhythms. Simulated AF dynamics and ablation target identification are significantly influenced by calibration data modality, highlighting the need for future research into patient-specific model calibration.

Acknowledgments

This research was funded by a UKRI Future Leaders Fellowship (MR/W004720/1) and used the ARCHER2 UK National Supercomputing Service (https://www.archer2.ac.uk). This work acknowledges the support of the National Institute for Health Research Barts Biomedical Research Centre (NIHR203330).

References

[1] Roney CH, Solis Lemus JA, Lopez Barrera C, Zolotarev A, Ulgen O, Kerfoot E, Bevis L, Misghina S, Vidal Horrach C, Jaffery OA, et al. Constructing bilayer and volumetric atrial models at scale. Interface Focus 2023;13(6):20230038.

[2] Horrach CV, Bevis L, Nwanna C, Zolotarev AM, Ehnesh M, Misghina SB, Al-Aidarous S, Honarbakhsh S, Roney CH. Atrial fibrosis in atrial fibrillation: Mechanisms, mapping techniques and clinical applications. The Journal of Physiology 2025;.

[3] Razeghi O, Solís-Lemus JA, Lee AW, Karim R, Corrado C, Roney CH, de Vecchi A, Niederer SA. Cemrgapp: An interactive medical imaging application with image processing, computer vision, and machine learning toolkits for cardiovascular research. SoftwareX 2020;12:100570.

[4] Fedorov A, Beichel R, Kalpathy-Cramer J, Finet J, Fillion-Robin JC, Pujol S, Bauer C, Jennings D, Fennessy F, Sonka M, et al. 3d slicer as an image computing platform for the quantitative imaging network. Magnetic Resonance Imaging 2012;30(9):1323–1341.

[5] Yushkevich PA, Piven J, Cody Hazlett H, Gimpel Smith R, Ho S, Gee JC, Gerig G. User-guided 3D active contour segmentation of anatomical structures: Significantly improved efficiency and reliability. NeuroImage 2006;31(3):1116–1128.

[6] Zolotarev A, Johnson K, Khan A, Slabaugh G, Roney C. An ensemble of 3d residual encoder unet models for solving multi-class bi-atrial segmentation challenge. In International Workshop on Statistical Atlases and Computational Models of the Heart. Springer, 2024; 209–213.

[7] Plank G, Loewe A, Neic A, Augustin C, Huang YL, Gsell MA, Karabelas E, Nothstein M, Prassl AJ, Sánchez J, et al. The opencarp simulation environment for cardiac electrophysiology. Computer Methods and Programs in Biomedicine 2021;208:106223.

[8] Labarthe S, Bayer J, Coudière Y, Henry J, Cochet H, Jaïs P, Vigmond E. A bilayer model of human atria: Mathematical background, construction, and assessment. Europace 2014; 16(suppl_4):iv21–iv29.

[9] Roney CH, Pashaei A, Meo M, Dubois R, Boyle PM, Trayanova NA, Cochet H, Niederer SA, Vigmond EJ. Universal atrial coordinates applied to visualisation, registration and construction of patient-specific meshes. Medical Image Analysis 2019;55:65–75.

[10] Coveney S, Roney CH, Corrado C, Wilkinson RD, Oakley JE, Niederer SA, Clayton RH. Calibrating cardiac electrophysiology models using latent gaussian processes on atrial manifolds. Scientific Reports 2022;12(1):16572.

[11] Courtemanche M, Ramirez RJ, Nattel S. Ionic mechanisms underlying human atrial action potential properties: Insights from a mathematical model. American Journal of Physiology Heart and Circulatory Physiology 1998; 275(1):H301–H321.

[12] Roney CH, Bayer JD, Cochet H, Meo M, Dubois R, Jaïs P, Vigmond EJ. Variability in pulmonary vein electrophysiology and fibrosis determines arrhythmia susceptibility and dynamics. PLoS Computational Biology 2018; 14(5):e1006166.

[13] Roney CH, Beach ML, Mehta AM, Sim I, Corrado C, Bendikas R, Solis-Lemus JA, Razeghi O, Whitaker J, O'Neill L, et al. In silico comparison of left atrial ablation techniques that target the anatomical, structural, and electrical substrates of atrial fibrillation. Frontiers in Physiology 2020;11:1145.

[14] Roney CH, Cantwell CD, Qureshi NA, Chowdhury RA, Dupont E, Lim PB, Vigmond EJ, Tweedy JH, Ng FS, Peters NS. Rotor tracking using phase of electrograms recorded during atrial fibrillation. Annals of Biomedical Engineering 2017;45(4):910–923.

[15] Beach M, Sim I, Mehta A, Kotadia I, O'Hare D, Whitaker J, Solis-Lemus JA, Razeghi O, Chiribiri A, O'Neill M, et al. Using the universal atrial coordinate system for mri and electroanatomic data registration in patient-specific left atrial model construction and simulation. In International Conference on Functional Imaging and Modeling of the Heart. Springer, 2021; 629–638.

[16] Vigmond E, Pashaei A, Amraoui S, Cochet H, Hassaguerre M. Percolation as a mechanism to explain atrial fractionated electrograms and reentry in a fibrosis model based on imaging data. Heart Rhythm 2016;13(7):1536–1543.

[17] Roney CH, Bayer JD, Zahid S, Meo M, Boyle PM, Trayanova NA, Haïssaguerre M, Dubois R, Cochet H, Vigmond EJ. Modelling methodology of atrial fibrosis affects rotor dynamics and electrograms. EP Europace 2016; 18(suppl_4):iv146–iv155.

[18] Honarbakhsh S, Horrach CV, Lambiase PD, Roney C, Hunter RJ. The effect of fixed and functional remodelling on conduction velocity, wavefront propagation, and rotational activity formation in atrial fibrillation. Europace 2024;26(10):euae239.

[19] Cantwell CD, Roney CH, Ng FS, Siggers JH, Sherwin SJ, Peters NS. Techniques for automated local activation time annotation and conduction velocity estimation in cardiac mapping. Computers in Biology and Medicine 2015; 65:229–242.

Address for correspondence:

Caroline Helen Roney
Digital Environment Research Institute (DERI), Empire House, 67-75 New Road, London, E1 1HH, United Kingdom
c.roney@qmul.ac.uk